Joint inversion of airborne gravity gradiometry and magnetic data from the Lac de Gras region of the Northwest Territories of Canada

Yue Zhu, University of Utah, Martin Čuma, University of Utah and TechnoImaging, Yuri Kinakin, RioTinto, and Michael S. Zhdanov, University of Utah and TechnoImaging*

Summary

This paper develops a method of joint inversion of airborne gravity gradiometry and magnetic data using Gramian constraints. The joint inversion technique reduces the non-uniqueness in the potential field inversion. The Gramian constraints make it possible to consider different correlations between multimodal geophysical parameters. The model study demonstrates that the joint inversion produces better results if one uses a logarithmic relationship between the density and magnetic susceptibility instead of a linear one. In the case of a body with strong remnant magnetization, one should consider inverting for the magnetization vector instead of a simple susceptibility inversion. This situation has been analyzed with both model and case studies. The case study includes joint inversion of airborne gravity gradiometry and magnetic data from the Lac de Gras region of the Northwest Territories of Canada, where the target kimberlites are characterized by strong remnant magnetization.

Introduction

One of the most challenging problems of the inversion of potential field data is its non-uniqueness. Joint inversion is one of the techniques capable of solving this problem by recovering more than one physical property jointly from a multimodal geophysical data. It is often the case in mature mining districts that there are several independent data sets available within the survey area, which makes the joint inversion more feasible and cost effective.

Different geophysical data sets are sensitive to different physical properties. The first challenge in any joint inversion is that one has to make an assumption about the relationship between the different properties. The direct joint parameter inversion method assumes a direct functional relationship between the different parameters (Heincke et al., 2006; Jegen et al., 2009). The cross-gradient constraint enforces the structural similarities between the different properties (Gallardo and Meju, 2003). Zhdanov et al. (2012) introduced the Gramian constraint, which can be treated as a generalized correlation between the different parameters. By specifying a type of Gramian constraints, one can enforce polynomial, gradient, or any other complex correlations.

It was demonstrated in a paper by Zhu et al. (2013) that the joint inversion algorithm worked well in the presence of linear and quadratic relationships between density and magnetic susceptibility. In practice, however, we often encounter a linear relationship between the density and the log of susceptibility (instead of a direct linear correlation between these two parameters). This paper shows how the joint inversion algorithm improves the inversion result in the case of the log relationship.

In the case of a strong remnant magnetization, one should consider an inversion for the magnetization vector instead of the magnetic susceptibility. Strong remanence can occur in such varied geological cases as kimberlites, dykes, iron-rich ultramafic pegmatitoids, platinum group element reefs, and banded iron formations. This paper provides an example of a model study of the effects of remnant magnetization on magnetization vector inversion. In the case study, we present an example of exploration for diamond-bearing kimberlites which show strong remnant magnetization. The joint inversion algorithm helps us locate the kimberlite zones, the results of which agree well with the local geology.

Principles of joint inversion using Gramian constraints

Let us consider forward geophysical problems for multiple geophysical data sets. These problems can be described by the following operator relationships:

$$d^{(i)} = A^{(i)}\left(m^{(i)}\right), i = 1,2,3,\cdots,n; \qquad (1)$$

where, in a general case, $A^{(i)}$ is a nonlinear operator, $d^{(i)}$ $(i = 1,2,3,\cdots,n)$ are different observed data sets (which may have different physical natures and/or parameters), and $m^{(i)}$ $(i = 1,2,3,\cdots,n)$ are the unknown sets of model parameters.

Note that, in a general case, different model parameters may have different physical dimensions (e.g., density is measured in g/cm^3, resistivity is measured in Ohm-m, etc.). It is convenient to introduce the dimensionless weighted model parameters, $\widetilde{m}^{(i)}$, defined as follows:

$$\widetilde{m}^{(i)} = W_m^{(i)} m^{(i)},$$

where $W_m^{(i)}$ is the corresponding linear operator of model weighting (Zhdanov, 2002).

The Gramian of a system of model parameters $\widetilde{m}^{(1)}, \widetilde{m}^{(2)}, \cdots, \widetilde{m}^{(n-1)}, \widetilde{m}^{(n)}$ is introduced as a determinant, $G(\widetilde{m}^{(1)}, \widetilde{m}^{(2)}, \cdots, \widetilde{m}^{(n-1)}, \widetilde{m}^{(n)})$, of the Gram matrix of a

DOI http://dx.doi.org/10.1190/segam2014-0246.1

set of functions, $\tilde{m}^{(1)}, \tilde{m}^{(2)}, \cdots, \tilde{m}^{(n-1)}, \tilde{m}^{(n)}$ (Zhdanov et al., 2012). It provides a measure of correlation between the different model parameters or their attributes. By imposing the additional requirement minimizing the Gramian in regularized inversion, we obtain multimodal inverse solutions with enhanced correlations between the different model parameters or their attributes.

For a regularized solution of the inverse problem, we introduce a parametric functional with Gramian stabilizers,

$$P^{\alpha}\left(\tilde{m}^{(1)}, \tilde{m}^{(2)}, \cdots \tilde{m}^{(n)}\right) = \sum_{i=1}^{n} \left\| \tilde{A}^{(i)}\left(\tilde{m}^{(i)}\right) - \tilde{d}^{(i)} \right\|_D^2 + \alpha c_1 \sum_{i=1}^{n} S_{MN,MS,MGS}^{(i)} + \alpha c_2 G\left(\tilde{m}^{(1)}, \cdots, \tilde{m}^{(n)}\right), \quad (2)$$

where $\tilde{A}^{(i)}(\tilde{m}^{(i)})$ are the weighted predicted data,

$$\tilde{A}^{(i)}\left(\tilde{m}^{(i)}\right) = \mathrm{W}_d^{(i)} A^{(i)}\left(\tilde{m}^{(i)}\right), \quad (3)$$

α is the regularization parameter, and c_1 and c_2 are the weighting coefficients determining the weights of the different stabilizers in the parametric functional.

The terms $S_{MN}^{(i)}$, $S_{MS}^{(i)}$, and $S_{MGS}^{(i)}$ are the stabilizing functionals, based on minimum norm, minimum support, and minimum gradient support constraints, respectively (Zhdanov, 2009). The solution of the minimization problem for the parametric functional (2) with the Gramian stabilizers can be achieved by using the re-weighted conjugate gradient method, as discussed in Zhdanov et al., (2012). This algorithm requires the first derivative of the forward modeling operator.

In the case of two model parameters (e.g., density and magnetic susceptibility), the first variation of the Gramian constraint is computed as follows:

$$\frac{\partial G}{\partial \tilde{m}^{(1)}} = \mathbf{l}_G^{(1)} = \tilde{m}^{(1)}\left(\tilde{m}^{(2)}, \tilde{m}^{(2)}\right) - \tilde{m}^{(2)}\left(\tilde{m}^{(2)}, \tilde{m}^{(1)}\right),$$
$$\frac{\partial G}{\partial \tilde{m}^{(2)}} = \mathbf{l}_G^{(2)} = \tilde{m}^{(2)}\left(\tilde{m}^{(1)}, \tilde{m}^{(1)}\right) - \tilde{m}^{(1)}\left(\tilde{m}^{(1)}, \tilde{m}^{(2)}\right). \quad (4)$$

Model study

Logarithmic correlation between density and magnetic susceptibility

In the first model study, we investigated the case of a logarithmic correlation between density and magnetic susceptibility. A model was created, consisting of five pipe-like targets with anomalous density and susceptibility ranges simulating the kimberlite pipes. The dimensions of each were set at 100 m by 100 m by 200 m (length x width x depth) (Figures 1 and 2). To make the synthetic model more realistic, we increased the density and susceptibility with depth. We assumed the following linear relationship between the density and log of magnetic susceptibility:

$$\rho = c \cdot \log(\chi/\chi_b) + \rho_b.$$

In this model we set c = 0.29, ρ_b = 2.67, and $\chi_b = 0.005$. Generally, the anomalous density varies from 0.6 to 1.0 g/cc and the susceptibility from 0.03 to 0.15 SI. We assumed that the airborne gravity and magnetic survey was conducted over an area of 1 km by 1 km at a flight height of 50 m. The corresponding gravity and gravity tensor components (Gz, Gxx, Gyy, and Gzz), as well as the TMI data were computed and used for the inversion.

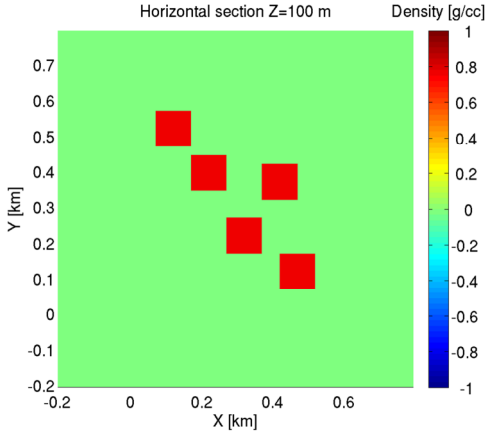

Figure 1: A horizontal section of the anomalous density distribution.

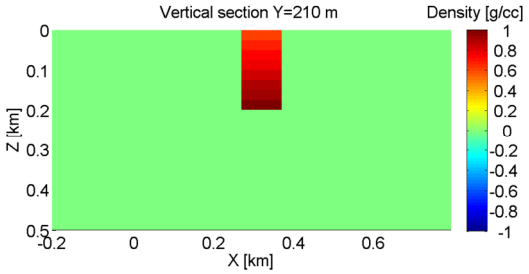

Figure 2: A vertical section of the anomalous density distribution.

The inversion domain has a dimension of 1 km by 1km by 500 m with the cell size of 25 m by 25 m by 25 m. The following transformed model parameters were used in the Gramian constraints:

$$Tm^{(1)} = \Delta\rho, Tm^{(2)} = \log\left(\frac{\chi}{\chi_b}\right).$$

Using the chain rule, we obtain the first variation of the Gramian constraint:

$$\frac{\partial G}{\partial \Delta\rho} = \frac{\partial G}{\partial Tm^{(1)}}, \qquad \frac{\partial G}{\partial \chi} = \frac{\partial G}{\partial Tm^{(2)}} \cdot \frac{\partial Tm^{(2)}}{\partial \chi}$$

After 100 iterations, the normalized misfit reached 3.5% for the gravity data and 0.74% for the magnetic data.

DOI http://dx.doi.org/10.1190/segam2014-0246.1

The horizontal and vertical sections of the predicted model are shown in Figures 3 to 6. The results obtained from the separate inversions are also provided. The joint inversion helped us recover higher anomalous density and susceptibility values, which were closer to the true model values. The depth resolution also appears to have been improved.

Joint inversion for density and magnetization vector

In this synthetic study, we jointly invert airborne gravity gradiometry and magnetic data in the presence of remnant magnetization. Model 2 represents a simple box model with dimensions of 500 m by 500 m by 200 m. The anomalous domain has a positive density anomaly of 0.5 g/cc and a constant magnetization vector, M, with the following scalar components: M = [1, 0, 1]. There is no magnetization in the background. We assumed that the airborne gravity and magnetic survey was conducted over an area of 1 km by 1 km at a flight height of 50 m.. All gravity gradiometry components and TMI data were simulated.

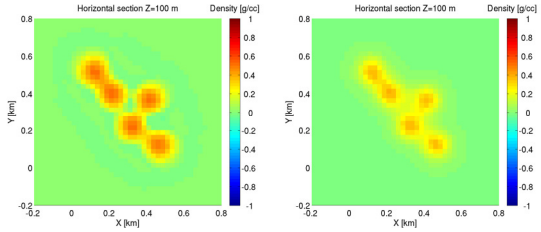

Figure 3: Horizontal sections of the anomalous density from the joint (the left panel) and separate (the right panel) inversions at Z=100 m.

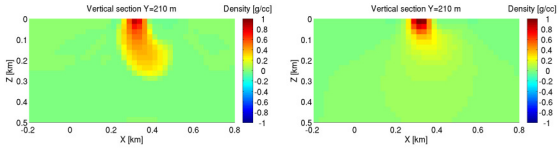

Figure 4: Vertical sections of the anomalous density from the joint (the left panel) and separate (the right panel) inversions.

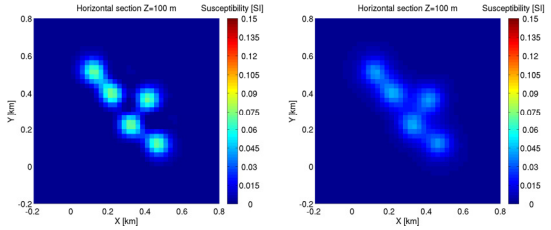

Figure 5: Horizontal sections of anomalous magnetic susceptibility from the joint (the left panel) and separate (the right panel) inversions at Z=100 m.

The inversion domain for this model study has a dimension of 1 km by 1 km by 700 m (length x width x depth) with a cell size of 25 m by 25 m by 25 m. In this case, the inversion was applied jointly for the anomalous density, $\Delta\rho$, and three components of the magnetization vector, M_x, M_y and M_z.

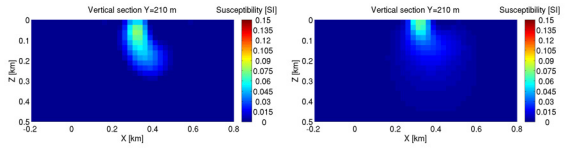

Figure 6: Vertical sections of the anomalous magnetic susceptibility from the joint (the left panel) and separate (the right panel) inversions.

Figure 7 shows the predicted magnitude of the magnetization vector obtained from the joint and discrete inversions. After applying the Gramian constraints, which enforce the correlation between density and absolute value of the magnetization vector, the recovered magnitude of the magnetization vector and the location of the anomaly were improved.

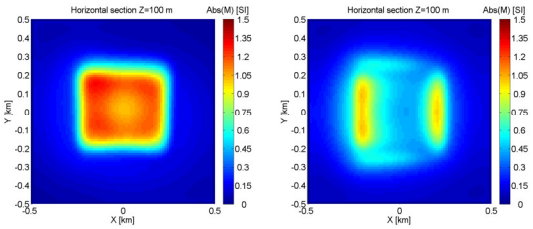

Figure 7: Horizontal sections of the magnitude of magnetization vector from the joint (the left panel) and separate (the right panel) inversions at a depth of 100 m. The joint inversion recovers a better shape and magnitude of the anomaly.

Case study in the Northwest Territories of Canada

We present a case study of the joint inversion of airborne gravity gradiometry and magnetic data collected in the Northwest Territories of Canada. The area of the survey belongs to the Slave Structural Province, which forms a distinct cratonic block within the Canadian Precambrian Shield. We have applied the aforementioned joint inversion method to airborne gravity gradiometry and magnetic data covering an area of 8 km by 7 km, with an average flights height of 33 m. This region has low topographic relief with variations of no more than 70 m. Both the total magnetic intensity (TMI) and all components of gravity tensor were collected. Figures 8 and 9 show the observed Gz and TMI data in the survey area. The gravity and gradiometry data used in the inversion were corrected for terrain effect using a reference density of 2.67 g/cc. The intensity of inducing field was subtracted from TMI data.

The joint inversion in this paper focuses on a subset of the data where kimberlites were accumulated. This subset covers the area outlined by the black box in Figure 9. The

DOI http://dx.doi.org/10.1190/segam2014-0246.1

inversion domain has a dimension of 2 km by 2 km by 1 km with the cell size of 25 m by 25 m by 25 m. We used Gz, Gxx, Gyy Gzz, and TMI data in the joint inversion. Since kimberlites in this region show strong remnant magnetization, we inverted the observed airborne data for density and the magnetization vector (as was done for Model 2). After 55 iterations, the normalized misfits decreased to 1.98% for the gravity data and to 0.1% for the magnetic data. Horizontal slices of predicted anomalous density at a depth of 100 m are shown in the top left panel in Figure 10. The top right panel shows the angle between the remnant and inducing parts of the magnetization vector at a depth of 100 m. The bottom two panels in Figure 10 display both the remnant and total magnitudes of the magnetization vector at a depth of 50 m.

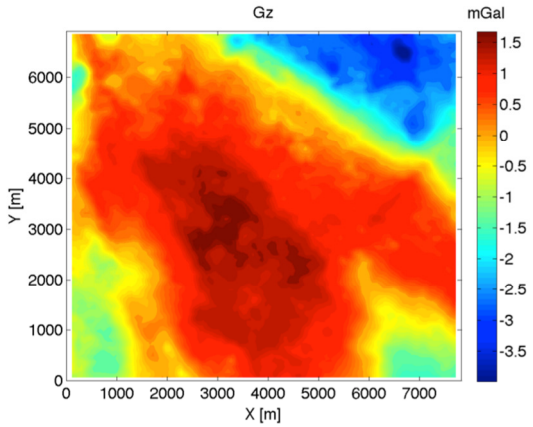

Figure 8: A map of the observed vertical gravity field Gz at the survey area.

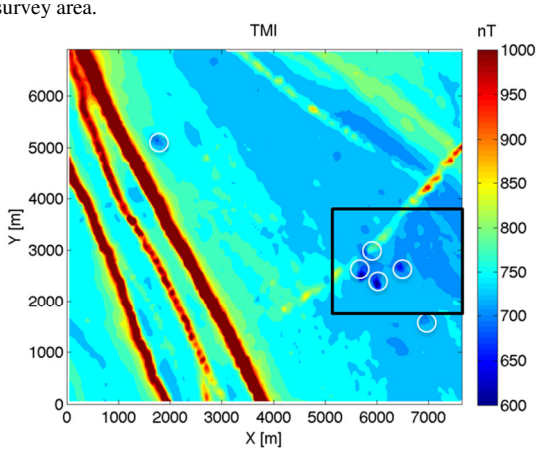

Figure 9: A map of the observed TMI data at the survey area. The white circles indicate the known kimberlite pipes. The black box indicates the area of the data subset used for inversion.

The circular anomalies in Figure 9 correspond to known kimberlite bodies. It is clear that the kimberlites correspond to the negative density anomalies and high magnitude of the magnetization vector, which agrees with the physical properties of the crater facies. The angle between remnant and induced magnetic vector seems to be a particularly good indicator of kimberlite. It is notable that, overall, the joint inversion algorithm overall recovered a higher magnitude for the magnetization vector.

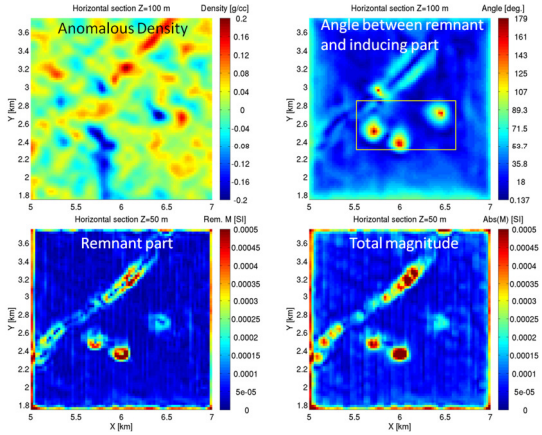

Figure 10: The case study: horizontal sections of anomalous density from the joint inversion (the left top panel), the angle between remnant and induced magnetization vector (the top right panel), the remnant part of the magnetization vector (the bottom left plane), and the total magnitude of the magnetization vector (the bottom right plane).

Conclusions

Using synthetic models, we have demonstrated that a joint inversion algorithm based on Gramian constraints is capable of improving inversion results in the case of a multi-dimensional dataset consisting of gravity and magnetic data. We have also shown that joint inversion for density and magnetization vectors works well in the presence of the significant remnant magnetization. The case study of joint inversion of magnetic and gravity gradiometry data in the Northwest Territories of Canada has demonstrated that joint inversion with Gramian constraints more accurately recovers the higher remnant magnetization typical of kimberlite pipes. The circular anomalies in the inverted dataset correspond well to the known kimberlite deposits.

Acknowledgements

The authors acknowledge CEMI and TechnoImaging for support of this research. We also acknowledge the Center for High Performance Computing, University of Utah, for providing computational resources. We also thank RioTinto for providing survey data and permission to publish the results.

DOI http://dx.doi.org/10.1190/segam2014-0246.1

http://dx.doi.org/10.1190/segam2014-0246.1

EDITED REFERENCES

Note: This reference list is a copy-edited version of the reference list submitted by the author. Reference lists for the 2014 SEG Technical Program Expanded Abstracts have been copy edited so that references provided with the online metadata for each paper will achieve a high degree of linking to cited sources that appear on the Web.

REFERENCES

Gallardo, L. A., and M. A. Meju, 2003, Characterization of heterogeneous near-surface materials by joint 2D inversion of DC resistivity and seismic data: Geophysical Research Letters, **30**, no. 13, doi: 10.1029/2003GL017370.

Heincke, B., M. Jegen, and R. Hobbs, 2006, Joint inversion of MT, gravity and seismic data applied to sub-basalt imaging: 76th Annual International Meeting, SEG, Expanded Abstracts, 784–789.

Jegen, M. D., R. W. Hobbs, P. Tarits, and A. Chave, 2009, Joint inversion of marine magnetotelluric and gravity data incorporating seismic constraints: Preliminary results of sub-basalt imaging off the Faroe Shelf: Earth and Planetary Science Letters, **282**, no. 1-4, 47–55, http://dx.doi.org/10.1016/j.epsl.2009.02.018.

Zhdanov, M. S., 2002, Geophysical inverse theory and regularization problems: Elsevier.

Zhdanov, M. S., 2009, New advances in regularized inversion of gravity and electromagnetic data: Geophysical Prospecting, **57**, no. 4, 463–478, http://dx.doi.org/10.1111/j.1365-2478.2008.00763.x.

Zhdanov, M. S., A. Gribenko, and G. Wilson, 2012, Generalized joint inversion of multimodal geophysical data using Gramian constraints: Geophysical Research Letters, **39**, no. 9, L09301, http://dx.doi.org/10.1029/2012GL051233.

Zhu, Y., M. S. Zhdanov, and M. Cuma, 2013, Gramian constraints in the joint inversion of airborne gravity gradiometry and magnetic data: 83rd Annual International Meeting, SEG, Expanded Abstracts, 1166–1170.